






Stability Analysis of Natural Slopes: Comparative Analysis Between the Strength Reduction and Stress Analysis Methods

**Análisis de estabilidad en taludes naturales:
análisis comparativo entre el método de reducción
de esfuerzos y análisis de tensión**

  Jonathan Vázquez García¹;
 Aldo Fernández Limés²

¹Universidad Tecnológica de La Habana
José Antonio Echeverría (CUJAE)
Havana-Cuba,
jonathavazgar@civil.cujae.edu.cu

²Universidad Tecnológica de La Habana
José Antonio Echeverría (CUJAE)
Havana-Cuba,
afernandezl@civil.cujae.edu.cu

How to cite / Cómo citar

J. Vázquez García, and A. Fernández Limés, "Stability Analysis of Natural Slopes: Comparative Analysis Between the Strength Reduction and Stress Analysis Methods," *Tecnológicas*, vol. 27, no. 61, e3164, 2024.

<https://doi.org/10.22430/22565337.3164>

Abstract

Natural slopes exhibit a variable cross-section, limiting the applicability of methods developed for regular slopes with constant cross-sections. This study aimed to compare the SAM and SRM methods by analyzing the stability of a slope with two inclinations (54° and 31°). The methodology involved obtaining a topographic surface and analyzing it using the MIDAS GTS NX program to demonstrate the influence of slopes and the analysis method on the factor of safety. The results showed that the influence of slopes is greater than that of the methods. Additionally, it was found that for small slopes, both methods yield similar results for small element sizes in the mesh, while for large slopes, the SAM method is less conservative, presenting values up to 130 % larger compared to SRM. Furthermore, the results obtained with the SAM method indicate that the steep slope is 13.7 % more stable than the gentle slope, which is not realistic. Additionally, the statistical analysis performed shows differences of -0.4 between the SAM and SRM methods on the steep slope, reinforcing the imprecision of the SAM method in obtaining the factor of safety in slopes with high inclinations compared to the SRM method. Therefore, it was concluded that the SRM method is much more effective than the SAM. In addition, it is recommended to use the SAM method as a complement to the SRM method for slopes with low inclinations.

Keywords

Factor of safety, midas software, slope stability, strength reduction method, stress analysis method.

Resumen

Las laderas naturales presentan una sección variable, lo que limita el uso de métodos que fueron desarrollados para taludes regulares de sección constante. Este estudio tuvo como objetivo la comparación de los métodos SAM y SRM a través del análisis de estabilidad de una ladera con dos pendientes (54° y 31°). La metodología consistió en la obtención de una superficie topográfica y su análisis empleando el programa MIDAS GTS NX, para demostrar la influencia de pendientes y del método de análisis en el factor de seguridad. Se obtuvo como resultado que la influencia de las pendientes es mayor que la de los métodos. Además, se obtuvo que, en pendientes pequeñas, ambos métodos presentan resultados semejantes para pequeños tamaños de elementos en la malla, mientras que, en grandes pendientes, el método SAM es menos conservador, presentando valores de hasta 130 % más grandes respecto al SRM. Además, los resultados obtenidos con el método SAM indican que la pendiente abrupta es un 13.7 % más estable que la suave, lo cual no es real. Además, el análisis estadístico realizado demuestra diferencias de -0.4 entre los métodos SAM y SRM en la pendiente abrupta, lo que refuerza la imprecisión del método SAM en la obtención del factor de seguridad en taludes con grandes pendientes con respecto al método SRM. Por lo tanto, se concluye con que el método SRM es mucho más efectivo que el SAM. Además, se recomienda emplear el método SAM como complemento del método SRM en laderas de poca inclinación.

Palabras clave

Factor de seguridad, software midas, estabilidad de taludes, método reducción de esfuerzos, método análisis de tensión.

1. INTRODUCTION

In the realm of geotechnical engineering, slope stability analysis holds immense significance in preventing landslides and soil mass detachments that could lead to human and material losses, this has prompted the investigation of this field through various studies [1]-[3]. These events can be triggered by the action of gravitational forces and seepage forces within the soil mass. In addition, they could fail due to excavation, the gradual disintegration of their structure, and could occur in almost any environment slowly or suddenly with or without apparent provocation [4]. Failures occur in various ways depending on the geological composition of the soil, and can occur in the form of falls, topples, slides, spreads, and flows [5].

Soil type, shape, and slope determine the risk level of slope collapse, which is quantified in what is known as the safety factor. The safety factor represents the local or global stability state of the slope, being in a critical state for safety factor values equal to 1 and unstable for lower values [6].

Since the early 20th century, various methods for evaluating slope stability have been developed, with the Limit Equilibrium Method (LEM) being the first among them and the most widely used [7]. According to [8], in the 1960s, with the advent of computers, the iterative processes characteristic of the aforementioned method was optimized, leading to increased research and the emergence of new proposals, due to that, in 1975, the Strength Reduction Method (SRM) was introduced by Zienkiewicz.

The SRM analyzes slope stability using the finite element method. This numerical analysis determines the minimum factor of safety and the failure mode by considering various loads and boundary conditions. Specifically, the SRM can be employed to simulate the failure process without any assumptions, resulting in a single failure surface [8].

The method consists of reducing the soil shear strength parameters through the use of a reduction factor. In this way, new strength parameters are obtained, which are reduced again by another factor [9]. This process is repeated progressively until the model reaches the limit equilibrium state and at that moment, the corresponding reduction factor is considered as the safety factor of the slope [9].

Furthermore, SRM determines the failure mechanism based on the zone where the soil mass is unable to withstand the applied stresses, leading to the automatic development of the potential failure surface. It can be applied in both two-dimensional and three-dimensional environments [10]. Its application has been studied in complex cases such as heterogeneous soils [11] and in scenarios where factors such as earthquakes, groundwater, and temperature are considered, as mentioned by [12], who conducted comparisons between this method and the Limit Equilibrium Method.

The SRM has also been employed by other researchers in the study of residual soils [13], which are soils that have not been mobilized by certain forces. It has also been used in studies on the hypoplasticity of clays [14], vegetated slopes [15], and various other applications [16], [17].

On the other hand, although the limit equilibrium method is one of the most widely used in current design to evaluate slope stability, this method does not allow determining the stress history in a real slope or the changes in soil behavior [18]. However, slope stability analysis using the finite element method can consider the slope formation process and other ground characteristics, but it requires more analysis time because it performs multiple nonlinear analyses [18].

In recent years, research have been carried out to combine the strengths of the limit equilibrium method and finite element-based slope stability analysis [19]-[21]. GTS NX

software offers a slope stability analysis method known as the Stress Analysis Method (SAM), which is a hybrid analytical method that combines the LEM and the finite element method and uses the results of the finite element stress analysis [18].

This method calculates the maximum strength of each element within the potential failure surface using the Mohr-Coulomb failure criterion. Therefore, similar to the SRM, this method can only be applied to constitutive models based on this criterion. Unlike the SRM, this method can only be employed in two-dimensional environments, and the potential failure surfaces within the soil mass must be predefined.

Many studies have shown that there are differences in the results obtained using analytical and numerical methods to evaluate slope stability [22], [23].

The objective of this study was to establish a comparison between two methods for evaluating slope stability, SRM and SAM, for which the MIDAS GTS NX program was used, where a mathematical calibration was applied to increase the accuracy of the results. The research starts with obtaining the topographic surface to be analyzed, from which two slopes of different slopes were extracted for study. These were analyzed three-dimensionally using the SRM method and then, cuts were made in the area where the maximum stresses are located to analyze the slope bidimensionally again with the SAM method and additionally with the SRM. Finally, the results obtained for the safety factors by both methods were compared.

2. MATERIALS AND METHODS

To evaluate two slope conditions, a topographic relief in the Tibetan region was selected. A real mountainous terrain occupying an area of 800 m² was selected and after obtaining the contour lines through the CADMAPPER website [24]-[27], the topography of the site was reproduced using the Autodesk Revit drawing tool, as shown in Figure 1.

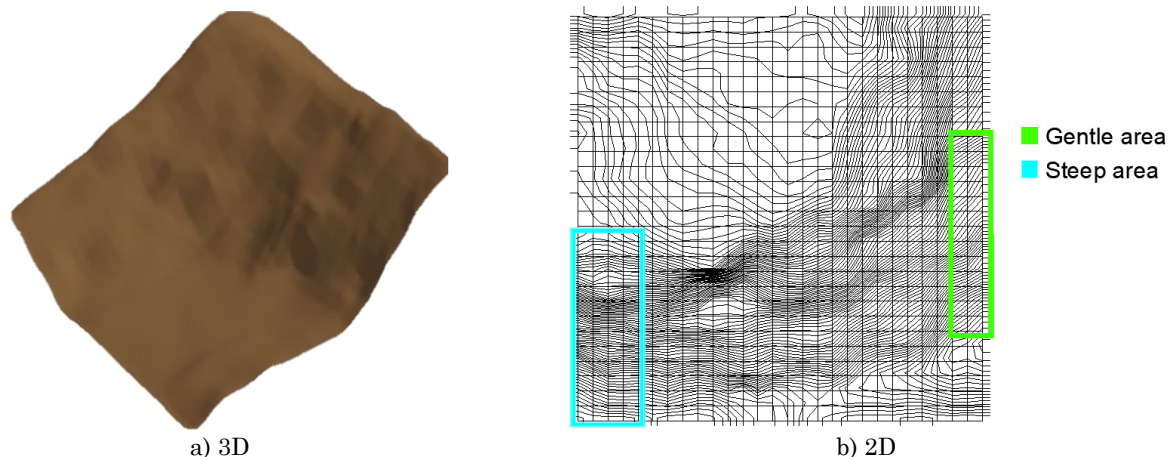


Figure 1. Topographic surface. Source: own elaboration.

The assumed soil mechanical properties were hypothetical, furthermore, the stratigraphic profile was considered homogeneous across the entire slope, consisting of a predominantly granular soil. With respect to its strength parameters, the soil exhibits a cohesion of 17.5 kPa and an internal friction angle of 36°. The soil's elastic modulus is 36500 kPa and its Poisson's ratio is 0.33. Finally, only the wet unit weight of the material (18.5 kN/m³) was considered, and the presence of the groundwater table was not taken into account. Also, the most widely

used constitutive model for this type of soil and conditions is the Mohr-Coulomb model [28]- [31].

For the analysis, the Midas GTS NX program was used, as it allowed for the representation and evaluation of the relief in a 3D space. In the Midas GTS NX program, the SRM and SAM methods were employed, as they were the only methods possible to evaluate in said program. To conduct a comparison between the two methods, the primary variable considered was the slope of the terrain. For this purpose, two similar areas were selected from the modeled terrain for analysis. One of the areas exhibits a slope of approximately 31° , henceforth referred to as "gentle," and the other area exhibits a slope of 54° , referred to as "steep" (Figure 1). The geometry of both areas is shown in Figure 2.

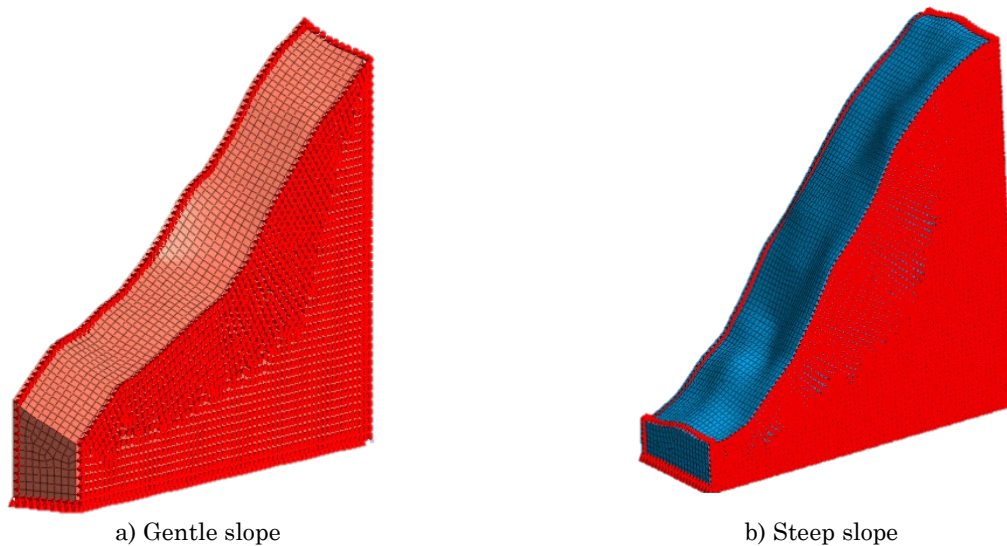


Figure 2. Slopes representation. Source: midas GTS NX (own elaboration).

2.1 Mathematical calibration

In three-dimensional models, only the SRM method can be employed. The control variables for calibrating the methods were: soil slopes, safety factors, mesh density, and computation time. To achieve stability of the results, a mathematical calibration process was carried out with 15 models for each surface, gradually reducing the size of the mesh elements from 20 m to 6 m, which was the minimum allowed by the installed computing capacity (Core i5, 16 GB RAM).

To obtain the most critical 2D models of the slope, cross-sections will be taken from the calibrated 3D models, where the maximum soil stresses are located. In the case of two-dimensional models, where both methods can be employed, the same procedure as for the three-dimensional model was used for the SRM method. On the other hand, in the SAM method, calibration was more complex due to the number of variables it encompasses. Unlike SRM, the SAM method is capable of providing infinite failure surfaces of the soil mass, which are calculated from two regions that must be drawn, which will be called "Center grid" and "Line grid". The first grid generates the centers of the soil failure curves, and it varies in width, length, slope, and the number of central points that are located. While the other grid determines the tangent lines to these circumferences, in the same way, it varies in width, length, slope, and the number of lines. The grids of the analysis are shown in Figure 3.

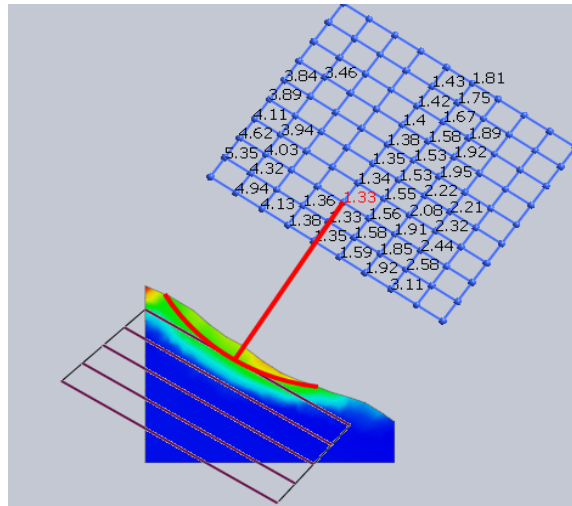


Figure 3. Grids representation. Source: midas GTS NX (own elaboration).

As can be observed, the Center Grid (blue) represents the center of the soil failure curve, while the Line Grid (red) represents the tangent lines to this curve.

Due to the large number of variables involved in the SAM method calibration, the calibration process was simplified. The slope and width of the Center grid were maintained as those corresponding to the slope being analyzed, and an element size of 20 m was maintained. First, the variables related to the Center grid (only length and number of centers) were calibrated, while the variables of the Line grid were kept constant. This process was repeated until stability was achieved in the model. Then, the Center grid was fixed, and the variables related to the Line grid were modified until total stability was achieved in the model. Once the optimal model was obtained, the element size of the meshes was reduced in the same way as for the SRM models to complete the calibration.

Computation time in the 2D environment was not considered as it was negligible for both the SRM and SAM methods. Tables 1, 2, 3 and 4 show the coding used to organize the grids within the SAM method during the calibration process.

Table 1. Steep slope Center grid encoding. Source: own elaboration.

Length	Number of points	Code
185	5	RA-1
185	8	RA-2
258	8	RA-3
258	10	RA-4
365	10	RA-5
365	15	RA-6
566	15	RA-7
566	30	RA-8
2327	50	RA-9
2327	100	RA-10

Table 2. Steep slope Line grid encoding. Source: own elaboration.

Width	Length	Number of lines	Slope	Code
179	505	3	-1.3	RA-11
179	505	5	-1.3	RA-12
179	505	8	-1.3	RA-13
179	505	20	-1.3	RA-14
209	439	20	-0.5	RA-15
132	506	20	-1.1	RA-16
147	535	20	-1.4	RA-17
147	535	50	-1.4	RA-18
179	505	3	-1.21	RA-19
179	505	5	-1.21	RA-20
208	603	8	-1.21	RA-21
208	603	20	-1.21	RA-22
209	509	8	-0.82	RA-23
182	506	8	-1.61	RA-24
213	581	20	-1.61	RA-25
213	581	50	-1.61	RA-26
163	479	20	-2.7	RA-27
163	479	50	-2.7	RA-28

Table 3. Gentle slope Center grid encoding. Source: own elaboration.

Length	Number of points	Code
372	10	RS-1
372	20	RS-2
372	50	RS-3
1208	50	RS-4
2500	50	RS-5

Table 4. Steep slope Line grid encoding. Source: own elaboration.

Width	Length	Number of lines	Slope	Code
400	171	5	0.863	RS-6
400	171	20	0.863	RS-7
400	200	20	0.863	RS-8
400	200	20	-1.2	RS-9
400	200	20	-0.5	RS-10

A greater number of models for the steep slope are presented in Tables 1 and 2 compared to the gentle slope. This is attributed to the attainment of stability in the results for the gentle slope occurring at a significantly faster rate than that for the steep slope.

The analysis can be performed using meshes with square, triangular, and hybrid (a combination of the two) elements. In the initial runs, the difference between the safety factors was less than 5 %. However, the computation time for the triangular mesh was 22 % higher than that for the hybrid mesh, due to the less structured nature of the triangular mesh. The rectangular mesh did not exhibit significant differences in computation time, but there were negligible differences of 4 % in the safety factors compared to the hybrid mesh. Therefore, the remaining two-dimensional and three-dimensional models were run using the hybrid

mesh, as it offered shorter computation times without significant differences in the safety factor.

2.2 3D model

The selection of the optimal domain (element size) is constrained by computation time and safety factors. Therefore, several runs were performed, progressively decreasing the element size in the three-dimensional models of both slopes. The safety factor values obtained for each slope are illustrated in Figure 4.

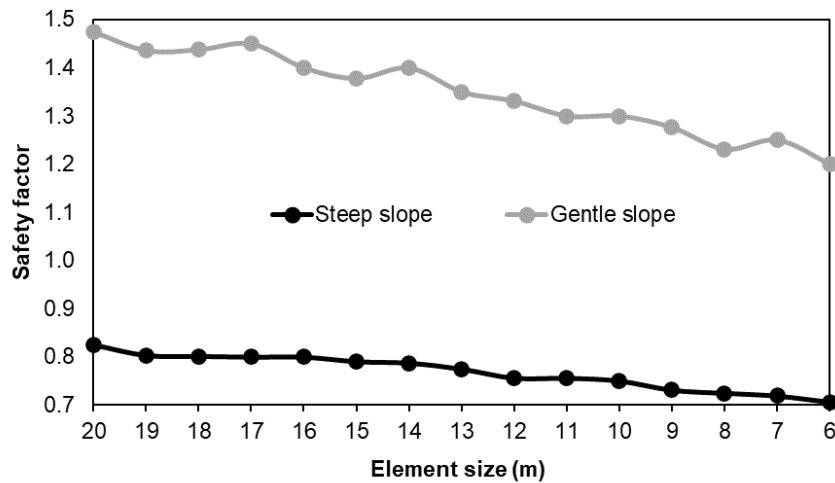


Figure 4. Safety factors for each 3D model. Source: own elaboration.

As can be observed in Figure 4, the behavior of both models is as expected. As the element size increased, the safety factor continued to decrease. For the gentle slope, values with minimal variation (less than 5 %) were obtained starting at an element size of 9 m. In addition, the steep slope model exhibited very stable behavior, with differences less than 5 % starting at an element size of 9 m. However, both models yielded relatively high computation time values compared to the other models. Figure 5 shows the computation time results obtained for each soil domain of both slopes.

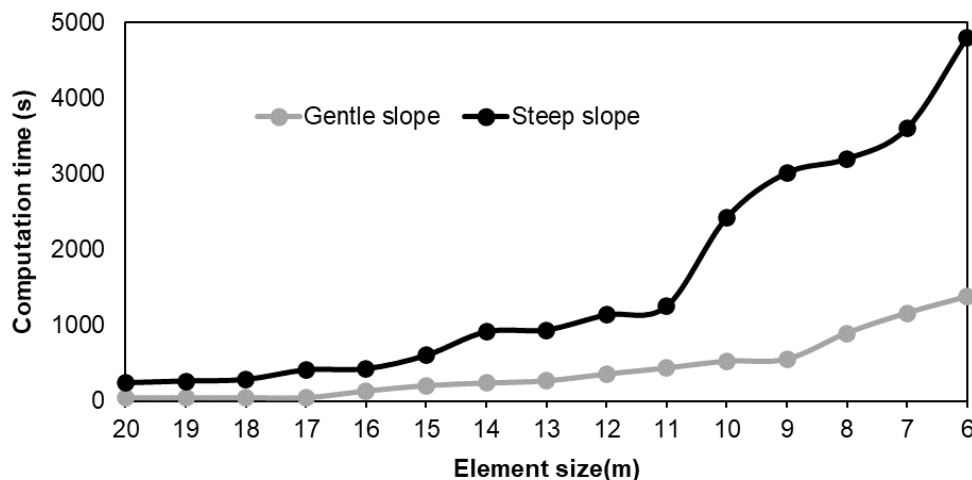


Figure 5. Computation time for each 3D model. Source: own elaboration.

As can be observed in Figure 5, starting from a mesh density of 9 m, the computation time for the gentle slope model begins to increase compared to the other models, with a difference of almost 60 % compared to the run with an element size of 6 m. On the other hand, for the steep slope model, the computation time increases rapidly starting from 11 m, with a difference of 80 % compared to the 6 m model.

For the gentle slope, the model corresponding to the element size of 9 m is adopted as the optimal one, since the safety factor error is less than 5 % and it has a computation time of 9 minutes. In the case of the steep slope, the 9 m model represents an increase in computation time of 25 % compared to the 10 m model; however, the error in the safety factor value of the 10 m model is 6.6 % compared to the 6 m model. Although the run time is longer, the 9 m model is selected in order to increase the accuracy of the results.

The failure surfaces for each slope will be obtained from the selected optimal models (element size of 9m in both cases); from these, the area of maximum stress will be selected to perform the 2D analysis (Figure 6).

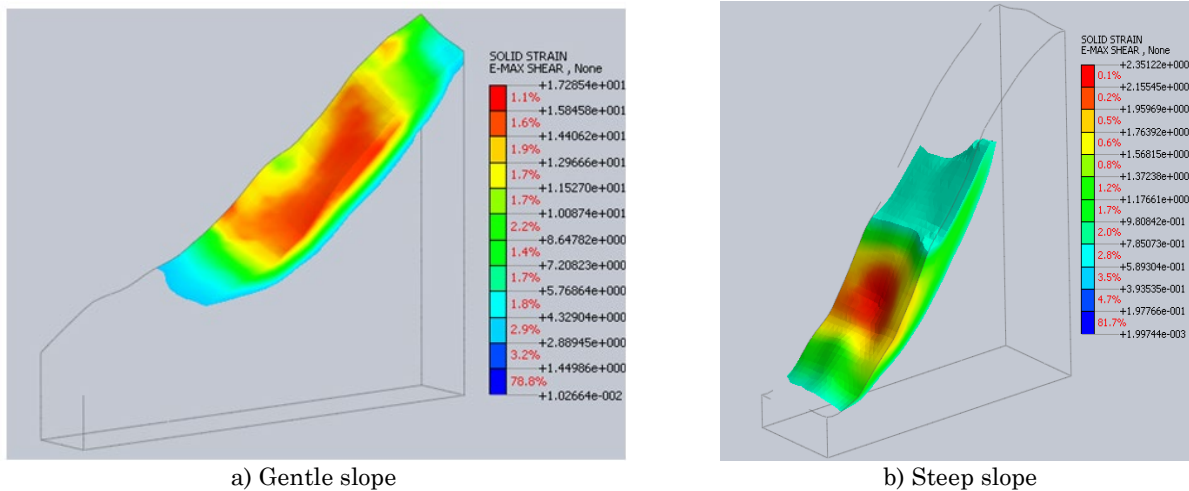


Figure 2. Soil stresses. Source: midas GTS NX (own elaboration).

2.3 2D model

With the sections where the maximum stresses of each slope were defined, it was possible to perform the analysis of the two-dimensional surfaces. In the SAM method, it was necessary to calibrate the meshes of both slopes. Next, Figure 7 shows the safety factor results for the steep slope for this calibration.

As can be observed in Figure 7, starting with the RA-19 model, the safety factors show a decreasing trend due to the change in slope of the line grid, reaching stability in the results with maximum variations of 2.48 % between the R-19 and R-22 models. The calibration was carried out with the RA-22 model, as it was with this model that the most critical safety factor was obtained. This model (RA-22) has 100 centers in the Center Grid and 20 lines in the Line Grid, with a slope of -1.21 %. Figure 8 shows the results for the gentle slope model.

In the case of the gentle slope, stability is observed in the results from the RS-2 model onwards, with the lowest values being obtained from the RS-6 model. Therefore, this model will be chosen for the remaining analyses. This model has 50 centers and 5 tangent lines with a slope of -0.86 %. Once the grid models for each slope were obtained, both 2D models were calibrated using the SRM and SAM methods.

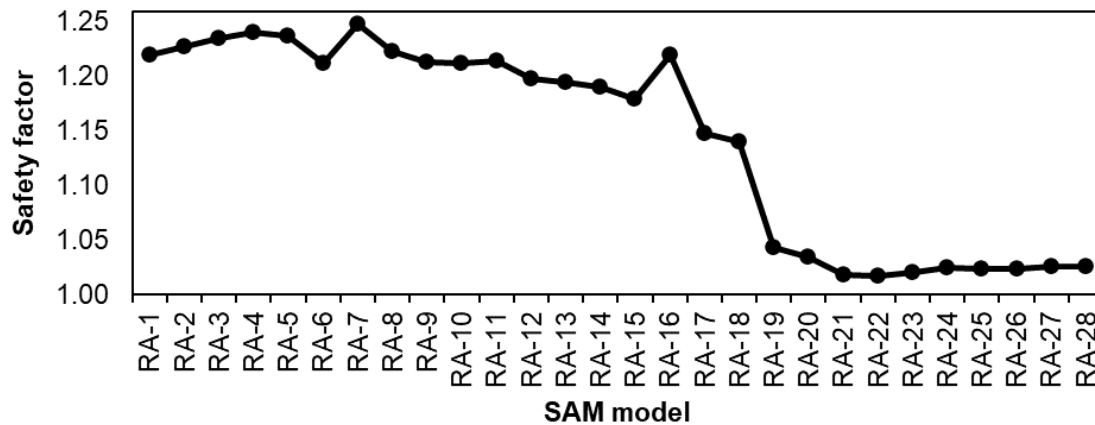


Figure 7. Steep slope grid calibration. Source: own elaboration.

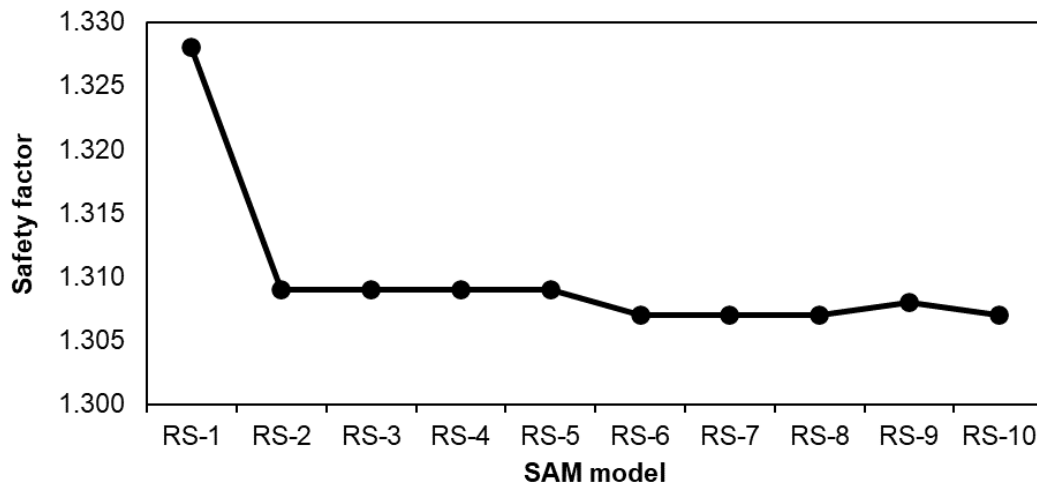


Figure 8. Gentle slope grid calibration. Source: own elaboration.

3. RESULTS AND DISCUSSION

A comparative analysis between both numerical methods for the two analyzed surfaces was carried out. Next, Figures 9 and 10 illustrate the comparison of the calibrations of the 3D models and the 2D models.

Observations from Figure 9 indicate a close resemblance between the 3D and 2D models employing the SRM method, with minor discrepancies in element sizes 17 and 14 meters, exhibiting differences of 6.9 % and 4.9 %, respectively. In contrast, the SAM model initially presents variations exceeding 10 %. However, from element size 13 onwards, the outcomes stabilize, and starting with mesh 8, the safety factors generated by both models converge, achieving a mere 3 % difference in meshes 8 and 6. Additionally the simple ANOVA indicated a difference of -0.019 within the SRM method, suggesting that the means are very similar. However, between SAM and SRM, there is a difference of -0.08, this indicates that the differences are statistically significant at the 95 % confidence level. Regardless of this ANOVA result, it is evident that as the element size grows, both models converge towards the same value. However, when those results are compared to studies by [23] and [4], it is found that these values do not coincide with the results obtained in the gentle slope.

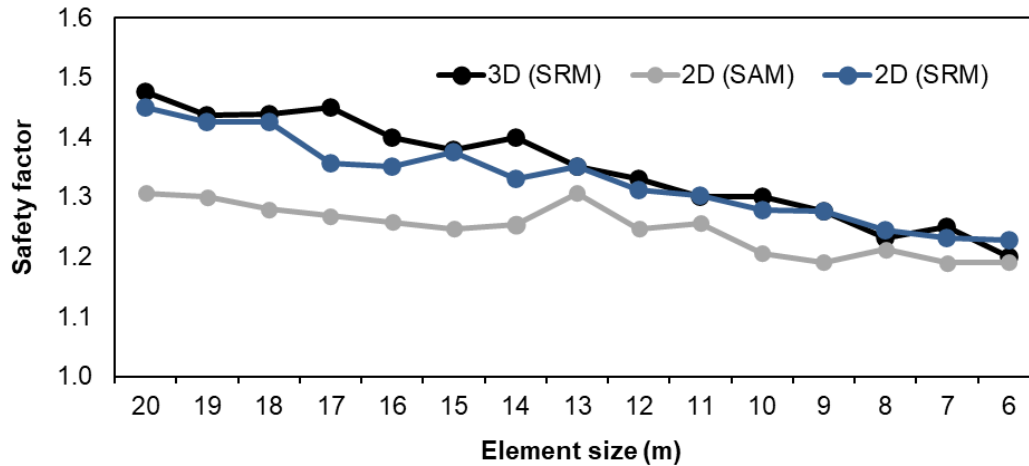


Figure 9. Gentle slope model comparison. Source: own elaboration.

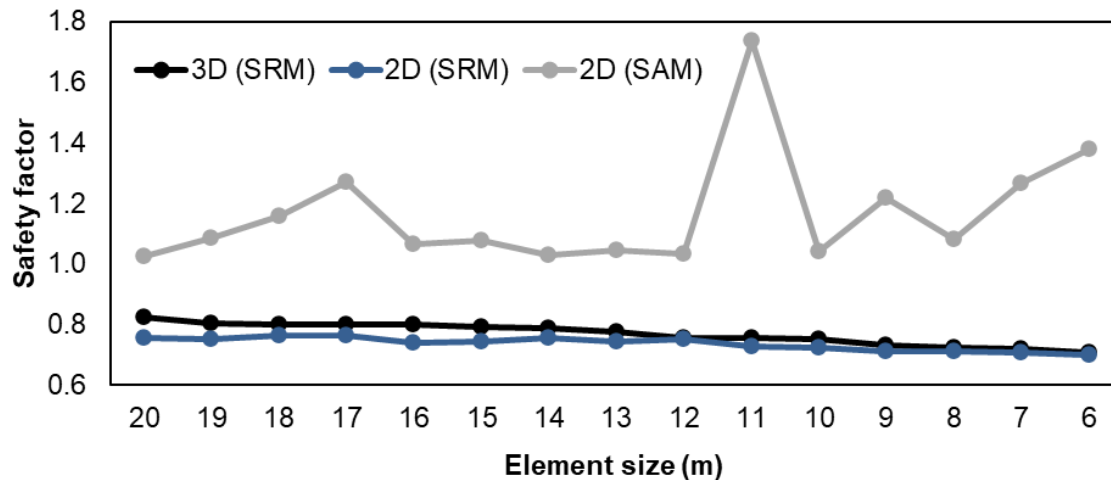


Figure 10. Steep slope model comparison. Source: own elaboration.

In this study, more conservative results are obtained with the analytical method, which does not correspond to the research carried out. This is due to the irregularity of the slope's cross-section, since most studies where analytical and numerical methods are compared to evaluate slope stability are only carried out on slopes with a regular section, as those made by [4], and other researches[22], [23].

Analogously to the previous case, in Figure 10 the outcomes obtained from the 3D and 2D models using the SRM method exhibit close agreement, with discrepancies diminishing further for grid sizes 14 and above, where the difference is merely 3.5 %. However, the disparity between the SAM and SRM methods is substantial, as the SAM method consistently yielded values that deviated significantly from those of the SRM method. The smallest discrepancy between the SAM and SRM methods was observed for grid sizes 20, 14, and 12. In these instances, the error exceeded 19.6 %, with the largest divergence occurring for the 11 m, where the SAM method yielded a value approximately 130 % higher than that of the SRM method. This is supported by the ANOVA analysis for a significance level of 95 %. A difference of -0.031 was found within the SRM method, while a difference of -0.4 was observed between SRM and SAM, highlighting the greater variability associated with the SAM method. Compared to the values obtained by [23], it is found that these values

correspond to those obtained in this study, since in both cases more conservative values are obtained with the numerical method. In addition, according to [23], the analytical methods show satisfactory safety factors, while in the simulation methods values are obtained where the safety factor is within an unsafe range, which corresponds to the analysis obtained in the steep slope. Consequently, the values produced by the SAM method in this case bear no resemblance to those obtained using the SRM method.

Furthermore, apart from the discrepancies observed between the SAM and SRM methods, the SAM method exhibits unstable behavior. This instability manifests as an increasing factor of safety with progressively larger grid sizes, leading to less conservative outcomes for more precise analyses. Additionally, the factor of safety achieved for the smallest grid size (6 m) is 1.38, which exceeds all values obtained by the SAM method for the gentle slope. This contradiction arises from the fact that a 54° slope is not 13.7 % more stable than a 31° slope when the only variable differentiating them is the slope angle. This highlights the limitations of the SAM method in accurately assessing the stability of natural slopes with steep inclinations.

A multi-factor ANOVA was employed to analyze the results, with factor of safety being the dependent variable. The independent variables included slope angle (31° and 51°) and the analysis methods (SAM and SRM in 2D, and SRM in 3D). The analysis revealed that, as anticipated, the variation in slope angle exerted a more pronounced influence on the factor of safety, with an effect size up to 14 times greater than that of the different analysis methods.

The obtained results are only affected by the analyzed control variables (soil properties, mesh density and computation time). Therefore, the results are specific only to the variables included in the study and it cannot be assumed that they apply to other variables that were not considered. The influence of the water table on slope stability or the heterogeneity of the terrain are factors that could influence the results if they were taken into account. However, the obtained results can be generalized as long as the soil are predominantly granular, homogeneous and exhibit a Mohr-Coulomb constitutive model. In addition, as long as the slopes are within the established range between a gentle slope (31°) and a steep slope (54°), the results obtained in the study will be valid.

4. CONCLUSIONS

This study aimed to calibrate a slope stability model for natural slopes and compare the effectiveness of two methods: SAM (Stress Analysis Method) and SRM (Strength Reduction Method). The findings clearly demonstrate that SRM outperforms SAM for analyzing slopes with steep inclinations. This superiority is evident not only from the direct comparison but also from the SAM method's behavior on such slopes, where increasing precision leads to inflated safety factors. The SAM analysis reveals that the steep slope exhibits a 13.7 % greater factor of safety than the gentle slope, a result that is physically inconsistent given the homogeneous soil conditions. On the other hand, the factors of safety for the gentle slope were found to be stable using this method; however, the steep slope showed significant variability, with differences approaching 130 %. Also, the statistical analysis performed shows differences of -0.4 between the SAM and SRM methods on the steep slope. Moreover, SRM can determine the failure curve without prior knowledge of its location, while SAM generates an infinite number of curves. The primary advantage of SAM lies in its ability to detect local soil failures due to the infinite curves it produces, whereas SRM only identifies the global failure of the soil mass. Therefore, it is recommended to use SAM in conjunction with SRM

for slopes with gentle slopes but not for determining the safety factor of global failures on steep slopes.

5. ACKNOWLEDGEMENT AND FUNDING

The study was conducted without financial support.

CONFLICTS OF INTEREST

The authors declare that there is no conflict of interest.

AUTHOR CONTRIBUTIONS

Jonathan Vázquez García: Conceptualization, methodology, investigation, writing-original draft.

Aldo Fernández Limés: Conceptualization, methodology, investigation, writing-review and editing, supervision.

6. REFERENCES

- [1] J. A. Sánchez Fornia, and J. Vaunat, "Análisis de la estabilidad de laderas mediante Macro-Elementos," in *Taludes 2022: X Simposio Nacional sobre Taludes y Laderas Inestables*, 2022, vol. 978, pp. 666–673. <http://hdl.handle.net/2117/373828>
- [2] L. R. Alejano, I. Pérez-Rey, X. Estévez-Ventosa, M. Muñiz-Menéndez, and J. Arzúa, "Natural instability phenomena in granitic rock masses: slopes in decomposed granite, boulder fields and irregular large granitic boulders," *Bol. Geol. Min.*, vol. 132, no. 4, pp. 375–398, Dec. 2021. <https://doi.org/10.21701/bolgeomin.132.4.002>
- [3] C. Sanhueza Plaza, and L. Rodríguez Cifuentes, "Análisis Comparativo de métodos de cálculo de estabilidad de taludes finitos aplicados a laderas naturales," *Rev. Constr.*, vol. 12, no. 1, pp. 17–29, Apr. 2013. <http://dx.doi.org/10.4067/S0718-915X2013000100003>
- [4] A. Burman, S. P. Acharya, R. R. Sahay, and D. Maity, "A comparative study of slope stability analysis using traditional limit equilibrium method and finite element method," *Asian Journal of Civil Engineering*, vol. 16, no. 4, pp. 467–492, Jan. 2015. <https://www.researchgate.net/publication/274076368>
- [5] A. Mohan, A. K. Singh, B. Kumar, and R. Dwivedi, "Review on remote sensing methods for landslide detection using machine and deep learning," *Trans. Emerg. Telecommun. Technol.*, vol. 32, no. 7, Jun. 2021. <https://doi.org/10.1002/ett.3998>
- [6] Y. Ahangari Nanehkaran *et al.*, "Application of Machine Learning Techniques for the Estimation of the Safety Factor in Slope Stability Analysis," *Water*, vol. 14, no. 22, p. 3743, Nov. 2022. <https://doi.org/10.3390/w14223743>
- [7] S. Ullah, M. U. Khan, and G. Rehman, "A Brief Review of the Slope Stability Analysis Methods," *Geological Behavior*, vol. 4, no. 2, pp. 73–77, 2020. <https://doi.org/10.26480/gbr.02.2020.73.77>
- [8] W. Fu, and Y. Liao, "Non-linear shear strength reduction technique in slope stability calculation," *Computers and Geotechnics*, vol. 37, no. 3, pp. 288–298, Apr. 2010. <https://doi.org/10.1016/j.compgeo.2009.11.002>
- [9] W. Gao, X. Chen, X. Wang, and C. Hu, "Novel strength reduction numerical method to analyse the stability of a fractured rock slope from mesoscale failure," *Eng. Comput.*, vol. 37, no. 4, pp. 2971–2987, Oct. 2021. <https://doi.org/10.1007/s00366-020-00984-2>
- [10] A. P. Dyson, and A. Tolooiyan, "Optimisation of strength reduction finite element method codes for slope stability analysis," *Innovative Infrastructure Solutions*, vol. 3, no. 1, p. 38, Apr. 2018. <https://doi.org/10.1007/s41062-018-0148-1>

- [11] Z. Nie, Z. Zhang, and H. Zheng, "Slope stability analysis using convergent strength reduction method," *Engineering Analysis with Boundary Elements*, vol. 108, pp. 402-410, Nov. 2019. <https://doi.org/10.1016/j.enganabound.2019.09.003>
- [12] W. Yuan, B. Bai, L. Xiao-chun, and W. Hai-bin, "A strength reduction method based on double reduction parameters and its application," *Journal of Central South University*, vol. 20, no. 9, pp. 2555-2562, Sep. 2013. <https://doi.org/10.1007/s11771-013-1768-4>
- [13] X. Jin, Y. Hua, and Q. Tang, "Applying the strength reduction method to study of stability of residual mountains: A particular application," *3C Tecnol. Glosas Innov. Apl. Pyme.*, vol. 12, no. 1, pp. 33-52, Jan. 2023. <https://doi.org/10.17993/3ctecno.2023.v12n1e43.33-52>
- [14] T. Kadlicek, and D. Mašín, "The strength reduction method in clay hypoplasticity," in *Lecture Notes in Civil Engineering*, Cham: Springer International Publishing, 2021, pp. 456-464. https://doi.org/10.1007/978-3-030-64514-4_44
- [15] B. Świtala, "Strength reduction method in the stability assessment of vegetated slopes," *Architecture, Civil Engineering, Environment*, vol. 16, no. 2, pp. 151-159, Mar. 2023. <https://intapi.sciendo.com/pdf/10.2478/acee-2023-0024>
- [16] Y. Rui, L. Jiacheng, B. Xuemeng, and Z. Cheng, "Stability analysis of rock slopes using the interface contact model and strength reduction method," *Frontiers in Earth Science*, vol. 10, Feb. 2023. <https://doi.org/10.3389/feart.2022.1118935>
- [17] X. Zaixian, L. Chao, F. Fang, and W. Fufei, "Study on the Stability of Soil-Rock Mixture Slopes Based on the Material Point Strength Reduction Method," *Applied Sciences*, vol. 12, no. 22, p. 11595, Nov. 2022. <https://doi.org/10.3390/app122211595>
- [18] MIDAS. "midas GTS NX, software de elementos finitos para análisis geotécnicos en 2D y 3D." [midasoft.com](https://www.midasoft.com). Accessed: Apr. 1, 2024. [Online]. Available: <https://www.midasoft.com/es/latinoamerica/productos/geotecnica/midasgtsnx>
- [19] Z. Renato, E. Luca, F. Paolo, P. Simone, T. Elena, and V. Minutolo, Lower bound limit analysis through discontinuous finite elements and semi-analytical procedures, in *Theoretical and Applied Mechanics: AIMETA 2022*, M. Di Paola, L. Fratini, F. Micari, and A. Pirrotta, Eds., Millersville PA, USA: Materials Research Forum LLC, 2023. https://books.google.com.co/books?hl=es&lr=&id=IaO3EAAAQBAJ&oi=fnd&pg=PA139&dq=Lower+bound+limit+analysis+through+discontinuous+finite+elements+and+semi-analytical+procedures&ots=J3x4Hcgl7&sig=NYoI5opQejOra6GsQCSJbl7tA1o&redir_esc=v#v=onepage&q=Lower%20bound%20limit%20analysis%20through%20discontinuous%20finite%20elements%20and%20semi-analytical%20procedures&f=false
- [20] S. Liu, and L. Shao, "Limit equilibrium conditions and stability analysis for soils," in *Proceedings of GeoShanghai 2018 International Conference: Fundamentals of Soil Behaviours*, A. Zhou, J. Tao, X. Gu, and L. Hu, Eds., Singapore: Springer Singapore, 2018, pp. 92-100. https://www.doi.org/10.1007/978-981-13-0125-4_10
- [21] F. Sengani, and F. Mulenga, "Application of Limit Equilibrium Analysis and Numerical Modeling in a Case of Slope Instability," *Sustainability*, vol. 12, no. 21, Oct. 2020. <https://www.doi.org/10.3390/SU12218870>
- [22] K. J. Agbelele, E. C. Houehanou, M. F. Ahlinhan, A. W. Ali, and H.C. Aristide, "Assessment of Slope Stability by the Fellenius Slice Method: Analytical and numerical approach," *World Journal of Advanced Research and Reviews*, vol. 18, no. 2, pp. 1205-1214, May. 2023. <https://wjarr.com/sites/default/files/WJARR-2023-0874.pdf>
- [23] J. Briceño *et al.*, "Análisis comparativo de estabilidad en taludes utilizando métodos comprobados y modelos numéricos de simulación," *Revista Ciencia e Ingeniería*, vol. 42, no. 1, pp. 63-70, Dec-Mar. 2021. <http://erevistas.saber.ula.ve/index.php/cienciaingenieria/article/view/16646>
- [24] A. A. Kareem, B. K. Oleiwi, and M. J. Mohamed, "Planning the Optimal 3D Quadcopter Trajectory Using a Delivery System-Based Hybrid Algorithm," *International Journal of Intelligent Engineering and Systems*, vol. 16, no. 2, Apr. 2023. <https://doi.org/10.22266/ijies2023.0430.34>
- [25] A. A. Kareem, M. J. Mohamed, and B. K. Oleiwi, "Unmanned aerial vehicle path planning in a 3D environment using a hybrid algorithm," *Bulletin of Electrical Engineering and Informatics*, vol. 13, no. 2, pp. 905-915, Apr. 2024. <https://beei.org/index.php/EEI/article/view/6020/3616>
- [26] P. Fejes, and A. Horkai, "Creating City Models in ArchiCAD Software Environment," *The International Journal of Engineering and Science (IJES)*, vol. 10, no. 1, pp. 11-17, Jan. 2021. <https://www.theijes.com/papers/vol10-issue1/C1001011117.pdf>
- [27] C. Carbonell-Carrera, J. L. Saorin, D. Melián-Díaz, and S. Hess-Medler, "Spatial Orientation Skill Performance with a Workshop Based on Green Infrastructure in Cities," *ISPRS International Journal of Geo-Information*, vol. 9, no. 4, p. 216, Apr. 2020. <https://doi.org/10.3390/ijgi9040216>

- [28] C. O. Aksoy, G. G. Uyar, and Y. Ozelik, "Comparison of Hoek-Brown and Mohr-Coulomb failure criterion for deep open coal mine slope stability," *Structural Engineering and Mechanics*, vol. 60, no. 5, pp. 809-828, Dec. 2016. <https://doi.org/10.12989/sem.2016.60.5.809>
- [29] A. V. R. Karthik, R. Manideep, and J. T. Chavda, "Sensitivity analysis of slope stability using finite element method.," *Innov. Infrastruct. Solut.*, vol. 7, no. 2, p. 184, Mar. 2022. <https://doi.org/10.1007/s41062-022-00782-3>
- [30] N. Latha, "Numerical Studies on Stability of Sand Slopes.," *ECS transactions*, vol. 107, no. 1, pp. 15309–15315, 2022. <https://doi.org/10.1149/10701.15309ecst>
- [31] W. Sun, G. Wang, and L. Zhang, "Slope stability analysis by strength reduction method based on average residual displacement increment criterion," *Bulletin of Engineering Geology and the Environment*, vol. 80, no. 6, pp. 4367-4378, Jun. 2021. <https://doi.org/10.1007/s10064-021-02237-y>